Chapter 2
Background Theory

This chapter reviews some of the fundamental electromagnetic principles for a basic understanding of metamaterials and metamaterials as terahertz modulator. Section 2.1 covers the basic electromagnetic properties of materials with non-positive dielectric parameters, permitivity (ϵ) and permeability (μ). In Sect. 2.2, basic Lorentz oscillator model for permitivity is developed to illustrate the anomalous dispersion behavior that is fundamental to the modulator design. Finally, the basic principle of wave modulation using metamaterials is formulated in Sect. 2.3.

Complete and rigorous electromagnetic analysis is beyond the scope of this book. For such in-depth analysis there is an excellent collection of standard textbooks such as Landau et al. [1], Jackson [2], Kong [3]. For detailed analysis on optical properties of materials, an excellent reference is Wooten [4]. For further exploration of metamaterials, readers are referred to texts on metamaterials such as Ramakrishna et al. [5], Tretyakov [6], Eleftheriades et al. [7], Caloz et al. [8], Engheta et al. [9], Pendry [10].

2.1 Plane Waves in a Nonconducting Medium

Material response to electromagnetic waves can fundamentally be expressed by the Maxwell equations at the atomic length scales. However, in most cases we are not interested in the fast variation of electric and magnetic fields at those microscopic scales, instead a macroscopic description is sufficiently accurate. At a macroscopic level, the Maxwell equations are written as

$$\nabla \cdot \mathbf{D} = \rho \tag{2.1}$$

$$\nabla \cdot \mathbf{B} = 0 \tag{2.2}$$

$$\nabla \times \mathbf{E} + \frac{\partial \mathbf{B}}{\partial t} = 0 \tag{2.3}$$

S. Rout, S. Sonkusale, *Active Metamaterials*, DOI 10.1007/978-3-319-52219-7_2

$$\nabla \times \mathbf{H} - \frac{\partial \mathbf{D}}{\partial t} = \mathbf{J} \tag{2.4}$$

where $\mathbf{E}$ and $\mathbf{H}$ are the macroscopic electric and magnetic fields, $\mathbf{D}$ is the displacement field and $\mathbf{B}$ is the magnetic induction. Similarly, $\mathbf{J}$ and $\mathbf{j}$ are the macroscopic net charge and current densities. These macroscopic expressions are averaged over lengths that is large compared to inter-molecular distance but still only a fraction of wavelength of the applied fields, resulting in a homogeneous approximation of the material. A detailed derivation of these equations from microscopic Maxwell equations can be found in Jackson [2].

The metamaterials discussed in this text can be macroscopically approximated as dielectrics or nonconductors that are a devoid of free charge, and the Maxwell equations (2.1)–(2.4) can be reduced to

$$\nabla \cdot \mathbf{D} = 0 \tag{2.5}$$

$$\nabla \cdot \mathbf{B} = 0 \tag{2.6}$$

$$\nabla \times \mathbf{E} + \frac{\partial \mathbf{B}}{\partial t} = 0 \tag{2.7}$$

$$\nabla \times \mathbf{H} - \frac{\partial \mathbf{D}}{\partial t} = 0 \tag{2.8}$$

In most materials, which are linear and isotropic, the displacement field $\mathbf{D}$ is directly proportional to the applied electric field $\mathbf{E}$:

$$\mathbf{D} = \epsilon \mathbf{E} \tag{2.9}$$

where ϵ which is dispersive, i.e., function of the frequency ω, $\mathbf{D} = \epsilon(\omega)\mathbf{E}$. The dispersion is associated with the inertia of the dipoles due to the mass of electrons. In addition to being dispersive, ϵ also requires to be a complex function on the account of causality where the imaginary part is attributed to the loss or the absorbed energy in the medium. For a succinct proof of ϵ as a dispersive and complex function, the reader is referred to Ramamkrishna et al. [5].

A similar analysis holds true for the magnetic permeability,

$$\mathbf{B} = \mu \mathbf{H} \tag{2.10}$$

where is μ is dispersive and a complex function as well.

The causality and analyticity domain of $\epsilon(\omega)/\epsilon_0$ allows the use of Cauchy's theorem to relate the real and the imaginary part of $\epsilon(\omega)/\epsilon_0$, known as the Kramers–Kronig relations, and is expressed as (Jackson [2])

$$\mathrm{Re}[\epsilon(\omega)/\epsilon_0] = 1 + \frac{1}{\pi} \mathrm{P} \int_{-\infty}^{\infty} \frac{\mathrm{Im}[\epsilon(\omega')/\epsilon_0]}{\omega' - \omega} d\omega' \tag{2.11}$$

$$\mathrm{Im}[\epsilon(\omega)/\epsilon_0] = -\frac{1}{\pi}\,\mathrm{P}\int_{-\infty}^{\infty}\frac{\mathrm{Re}[\epsilon(\omega')/\epsilon_0]-1}{\omega'-\omega}d\omega' \tag{2.12}$$

where P means the principal value of the Cauchy's integral. This relation is regarded as very fundamental to the dispersion nature of ϵ. This relation allows the calculation of $\mathrm{Re}[\epsilon(\omega)]$ from the experimental data of $\mathrm{Im}[\epsilon(\omega)]$ from absorption experiments.

For sinusoidal solutions ($e^{-i\omega t}$), the equations for the $\mathbf{E}(\omega, \mathbf{x})$,etc.

$$\begin{aligned} \nabla\cdot\mathbf{B} &= 0, \qquad \nabla\times\mathbf{E} - i\omega\mathbf{B} = 0 \\ \nabla\cdot\mathbf{D} &= 0, \qquad \nabla\times\mathbf{H} + i\omega\mathbf{D} = 0 \end{aligned} \tag{2.13}$$

For uniform isotropic linear media, $\mathbf{D} = \epsilon\mathbf{E}, \mathbf{B} = \mu\mathbf{H}$ where ϵ and μ in general maybe complex functions of ω. For real and positive ϵ and μ (no losses), $\mathbf{D}$ and $\mathbf{B}$ can be substituted in Eq. (2.13) to get the Helmholtz wave equation (See Appendix A.1)

$$\left(\nabla^2 + \mu\epsilon\omega^2\right)\left\{\begin{matrix}\mathbf{E}\\ \mathbf{B}\end{matrix}\right\} = 0 \tag{2.14}$$

A plane-wave solution, traveling in the x direction, that satisfies both the Maxwell's equation (2.13) and the Helmholtz's equation (2.14) can be shown to be

$$\begin{aligned} \mathbf{E}(\mathbf{x}, t) &= \mathbf{E}_0 e^{i(kx-\omega t)} \\ \mathbf{B}(\mathbf{x}, t) &= \mathbf{B}_0 e^{i(kx-\omega t)} \end{aligned} \tag{2.15}$$

where k is the wave number

$$k = \sqrt{\epsilon\mu}\,\omega \tag{2.16}$$

The *phase velocity* of the wave is

$$v = \frac{\omega}{k} = \frac{1}{\sqrt{\epsilon\mu}} = \frac{c}{n} \tag{2.17}$$

The quantity n is called the *index of refraction* that can be expressed as

$$n = \sqrt{\frac{\mu}{\mu_0}\frac{\epsilon}{\epsilon_0}} = \sqrt{\mu_r\epsilon_r} \tag{2.18}$$

The wave impedance Z can be expressed as

$$Z = \frac{E_0}{H_0} = \frac{k}{\omega\epsilon} = \frac{1}{v\epsilon} = \sqrt{\frac{\mu}{\epsilon}} = \zeta Z_0 \quad \zeta = \frac{\mu_r}{\epsilon_r} \tag{2.19}$$

2.1.1 Negative Refractive Index

It can be seen from Helmholtz's equation (2.14) that propagating waves exist in materials whether ϵ and μ are both positive or negative. In this equation, ϵ and μ enter as a product, so it would not appear to matter whether both the signs are positive or negative. Conventionally, we always express the refractive index n as $+\sqrt{\mu_r \epsilon_r}$ for positive materials ($\epsilon > 0, \mu > 0$).

But, one needs to be careful in taking the square root for $n = \pm\sqrt{\mu_r \epsilon_r}$, that is resolved by proper analysis. In real materials, the constitutive parameters (ϵ, μ) are complex quantities and causality requires the imaginary part to be positive since the materials are passive. For a left-handed material (LHM), the constitutive parameters satisfy

$$\begin{aligned} \epsilon_r &= e^{i\phi_\epsilon}, \quad \phi_\epsilon \in (\pi/2, \pi] \\ \mu_r &= e^{i\phi_\mu}, \quad \phi_\mu \in (\pi/2, \pi] \end{aligned} \tag{2.20}$$

and now the refractive index can be expressed as

$$n = \sqrt{\epsilon_r \mu_r} = e^{i\phi_\epsilon/2} e^{i\phi_\mu/2} \tag{2.21}$$

and causality requires the imaginary part of the each $\sqrt{\epsilon}$ and $\sqrt{\mu}$ be positive

$$n = (\epsilon_r' + i\epsilon_r'')(\mu_r' + i\mu_r'') \tag{2.22}$$

where $\epsilon_r' = \cos(\phi_\epsilon/2)$, $\epsilon_r'' = \sin(\phi_\epsilon/2)$, $\mu_r' = \cos\left(\phi_\mu/2\right)$ and $\mu_r'' = \sin\left(\phi_\mu/2\right)$.

If the real part of each of the complex quantity in Eq. (2.22) goes to zero, the positive imaginary values result in a real $n < 0$. Therefore,

$$n = -\sqrt{\epsilon_r \mu_r}, \quad \epsilon_r < 0, \mu_r < 0 \tag{2.23}$$

A detailed derivation of it can be found in [11, 12].

2.1.2 Propagation of Waves in Left-Handed Material

For plane monochromatic wave proportional to $\exp(ikx - i\omega t)$, Eqs. (2.1)–(2.4) along with $\mathbf{D} = \epsilon\mathbf{E}, \mathbf{B} = \mu\mathbf{H}$ reduce to [13] (See Appendix A.2)

$$\begin{aligned} \mathbf{k} \times \mathbf{E} &= \omega\mu\mathbf{H} \\ \mathbf{k} \times \mathbf{H} &= -\omega\epsilon\mathbf{E} \end{aligned} \tag{2.24}$$

It can be seen from these equations that for materials with $\epsilon > 0$ and $\mu > 0$ they form a right-handed triplet vectors and so the term *Right-Handed Materials* (RHM), and for materials with $\epsilon < 0$ and $\mu < 0$ they form a left-handed triplet vectors and so the term *Left-Handed Materials* (LHM).

This should not be confused with the left-handed chiral optical materials which are completely different. This has prompted authors to call these *backward wave media* [14], *negative phase velocity media* [12], *double negative media* [11] or *negative refractive index materials* [15].

The energy flux carried by the wave is determined by the Poynting vector **S**, given by

$$\mathbf{S} = \mathbf{E} \times \mathbf{H} \tag{2.25}$$

and the direction of the vector is given by the right-hand rule which is the same for right-handed materials. Since Poynting's Theorem is derived by considering conservation of energy [2], we can think of a matched interface of a right-handed material with a left-handed material and the energy flow has to be in the same direction. Therefore, according to Eq. (2.25) the vector **S** is in parallel with the wave vector **k** for right-handed materials and is anti-parallel for left-handed materials.

2.1.3 Propagation of Waves in Single Negative Medium

A single negative medium has either $\epsilon < 0$ or $\mu < 0$. For this analysis, we will assume $\epsilon < 0$ and $\mu = \mu_0$. The wave number k can be expressed as

$$k = \omega\sqrt{\mu_0|\epsilon_r|}e^{i\phi_e/2} = k' + ik'' \tag{2.26}$$

By substituting k (2.26) in a plane wave ($\mathbf{E}(x,t) = \mathbf{E}_0 e^{i(kx-\omega t)}$), it can be expanded to

$$\mathbf{E}(x,t) = e^{-k''x}\mathbf{E}_0 e^{i(k'x-\omega t)} \tag{2.27}$$

The analysis for $\mu < 0, \epsilon > 0$ is similar. Therefore, the propagating wave in a single negative media is a decaying wave front.

2.2 Dispersion in Nonconductors

In the previous section, it has been shown that the propagation of EM waves in nonconducting media is governed by two properties of the material, which was assumed to be constant: the permittivity ϵ, and the permeability μ. It is well known from optics that the *refractive index* ($n = c\sqrt{\epsilon\mu}$) is a function of ω. Thus a prism bends blue light more sharply than red, spreading white light into a rainbow of colors. This phenomena is called *dispersion* and whenever the speed of a wave varies

with frequency, the supportive medium is called *dispersive*. Although both ϵ and μ are function of ω, in practice, μ is very close to μ_0, for most natural materials, and its variation with ω is insignificant [16].

2.2.1 Lorentz Oscillator Model for Permitivity

The classical theory of the absorption and dispersion for nonconductors (insulators) is due mainly to Lorentz. The Drude model is applicable to free-electron metals. Although these models were based on classical ad hoc formulation, the quantum mechanical analogs are strikingly similar and to date, the Drude–Lorentz models are still very useful for developing a feel for optical properties of solids.

The Lorentz model considers an atom with electrons bound to the nucleus using a model described by a small mass tied to a large mass by spring. The motion of an electron is then described by

$$m\left[\ddot{\mathbf{x}} + \gamma\dot{\mathbf{x}} + \omega_0^2\mathbf{x}\right] = -e\mathbf{E}(\mathbf{x}, t) \tag{2.28}$$

where $m\gamma\dot{\mathbf{x}}$ is the damping force representing the energy loss mechanism which arises due to radiation from an atom due to different scattering mechanisms. The term $m\omega_0^2\mathbf{x}$ is the Hooke's law restoring force in the *electron oscillator* model. In the context of a classical model, there are two main assumptions in Eq. (2.28). The nucleus has been assumed to have infinite mass and the small magnetic force $-e\mathbf{v} \times \mathbf{B}/c$ on the electron due to the magnetic component has been neglected.

For a sinusoid electric field with frequency ω as $e^{-i\omega t}$, the displacement vector $\mathbf{x}$ is the solution of Eq. (2.28) and the dipole moment $\mathbf{p}$ contributed by each electron is [2]

$$\mathbf{p} = -e\mathbf{x} = \left[\left(\frac{e^2}{m_e}\right)\frac{1}{(\omega_0^2 - \omega^2) - i\omega\gamma}\right]\mathbf{E} = \xi(\omega)\mathbf{E} \tag{2.29}$$

where $\xi(\omega)$ is the frequency dependent atomic polarizability. Assuming a linear relationship between $\mathbf{p}$ and $\mathbf{E}$ due to small displacements, $\xi(\omega)$ is a complex quantity because of the damping term in the oscillator model.

For N atoms per unit volume, the macroscopic polarization is [4]

$$\mathbf{P} = N\langle\mathbf{p}\rangle = N\xi(\omega)\langle\mathbf{E}\rangle = \epsilon_0\chi(\omega)\mathbf{E} \tag{2.30}$$

where $\chi(\omega) = N\xi(\omega)/\epsilon_0$ is the frequency dependent complex susceptibility that is defined in relation to the constitutive parameters as

$$\mathbf{D} = \epsilon_0(1 + \chi(\omega))\mathbf{E} = \epsilon_0\epsilon_r(\omega)\mathbf{E} \tag{2.31}$$

Using Eqs. (2.29)–(2.31), the relative permitivity $\epsilon_r(\omega)$ is

$$\epsilon_r(\omega) = 1 + \frac{\omega_p^2}{(\omega_0^2 - \omega^2) - i\omega\gamma}, \qquad \omega_p^2 = \frac{Ne^2}{m_e\epsilon_0} \tag{2.32}$$

where ω_p is the plasma frequency of the insulator which is the oscillating frequency in Drude model where the restoring force term $m_e\omega\gamma$ is zero. In other words, the Drude model for metals is obtained directly from the Lorentz model for insulators simply by equating the restoring force to zero.

2.2.2 *Anomalous Dispersion and Resonant Absorption*

From the complex permitivity expression in Eq. (2.32), the real and imaginary part of $\epsilon_r = \epsilon_r' + i\epsilon_r''$ can be written as

$$\begin{aligned} \epsilon_r'(\omega) &= 1 + \omega_p^2 \frac{\omega_0^2 - \omega^2}{(\omega_0^2 - \omega^2)^2 + \omega^2\gamma^2} \\ \epsilon_r''(\omega) &= \omega_p^2 \frac{\omega\gamma}{(\omega_0^2 - \omega^2)^2 + \omega^2\gamma^2} \end{aligned} \tag{2.33}$$

where $\epsilon_r' = \mathtt{Re}[\epsilon_r]$ and $\epsilon_r'' = \mathtt{Im}[\epsilon_r]$. The imaginary part is directly associated with the absorption of the incident wave and also when the real part is negative. The frequency dependence of ϵ_r' and ϵ_r'' is plotted in Fig. 2.1. Except for a narrow region around the resonance, ϵ_r' increases with frequency called the normal dispersion. In the narrow region of the resonance it decreases with frequency called *anomalous dispersion*. This region is also the frequency interval of maximum absorption as will be shown later in this section. The width of this region is equal to the loss factor γ.

With ϵ now a complex function of ω, the dispersive medium admits x-polarized plane-wave solutions, as before,

$$\mathbf{E}(x,t) = \mathbf{E}_0 e^{i(kx - \omega t)} \tag{2.34}$$

However, the wave number $k = \omega\sqrt{\epsilon\mu}$ is complex, because ϵ is complex. Writing k in terms of real and imaginary parts of the refractive index

$$k = \beta + i\frac{\alpha}{2} \tag{2.35}$$

equation (2.34) becomes

$$\mathbf{E}(x,t) = \mathbf{E}_0 e^{-\alpha x/2} e^{i(\beta x - \omega t)} \tag{2.36}$$

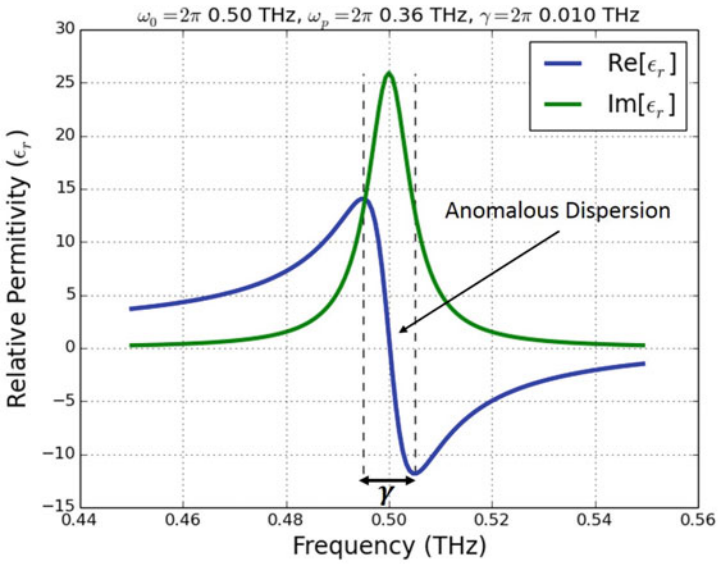

Fig. 2.1 Real and imaginary parts of the dielectric constant $\epsilon(\omega)/\epsilon_0$ in the neighborhood of a resonance. The region of anomalous dispersion is also the frequency interval for the maximum absorption

Evidently, $\alpha/2$ measures the *attenuation* of the wave. Because the *intensity* is proportional to E^2, it falls off as $e^{-\alpha x}$, α is called the *absorption coefficient*. For non-magnetic material ($\mu = \mu_0$), the complex frequency dependent refractive index n can be expressed as

$$n = n_R + in_I = \sqrt{\epsilon_r' + i\epsilon_r''} \tag{2.37}$$

where the n_R and n_I are the real and imaginary part of complex n known as the *ordinary refractive index* and *extinction coefficient*, respectively.

Squaring and equating both sides of Eq. (2.37) we get

$$\epsilon_r' = n_R^2 - n_I^2, \qquad \epsilon_r'' = 2n_R n_I \tag{2.38}$$

From Eq. (2.38), the real and imaginary part of the refractive index are

$$\begin{aligned} n_R &= \left\{ \frac{1}{2} \left[\sqrt{(\epsilon_r')^2 + (\epsilon_r'')^2} + \epsilon_r' \right] \right\}^{1/2} \\ n_I &= \left\{ \frac{1}{2} \left[\sqrt{(\epsilon_r')^2 + (\epsilon_r'')^2} - \epsilon_r' \right] \right\}^{1/2} \end{aligned} \tag{2.39}$$

Now, the absorption coefficient α can be expressed in terms of the refractive index using the relation

$$k = n\omega\sqrt{\epsilon_0\mu_0} = k_0\omega(n_R + in_I), \qquad k_0 = \sqrt{\epsilon_0\mu_0} \tag{2.40}$$

From Eq. (2.40) we can express the absorption coefficient as

$$\alpha = 2k_0\omega n_I \tag{2.41}$$

Typically, for analyzing absorption around the resonance, n_I is sufficient indicator since ω does not change appreciably in that region.

Another optical parameter that provides independent information about the material in the frequency of interest is the reflection coefficient. From Eq. (2.39), the reflection coefficient at normal incidence is given by Wooten [4]

$$R = \frac{(n_R - 1)^2 + n_I^2}{(n_R + 1)^2 + n_I^2} \tag{2.42}$$

The plots for the real/imaginary part of the refractive index [Eq. (2.39)] and the reflection coefficient [Eq. (2.42)] are shown in Fig. 2.2. From the plots, we can see the implications of the frequency dependence of ϵ_r' and ϵ_r''. The plots show four distinct regions, transmission, absorption, reflection, and transmission again.

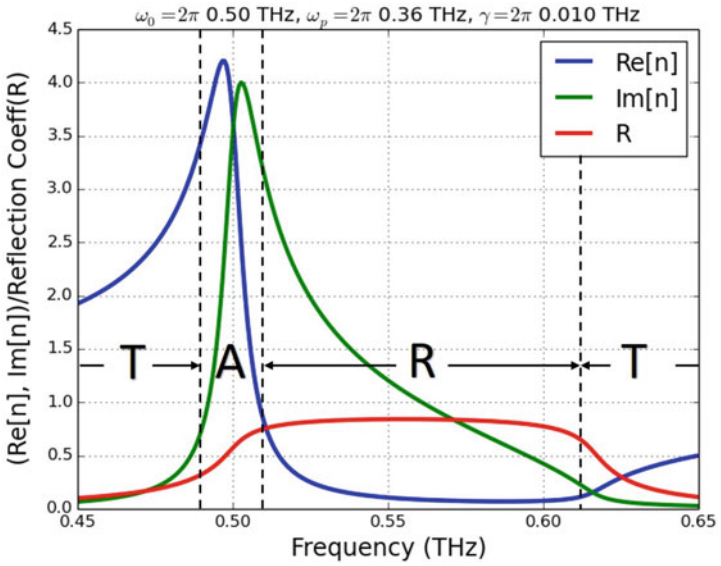

Fig. 2.2 Plots of the real and imaginary part of the refractive index [Eq. (2.39)] and the reflection coefficient [Eq. (2.42)] for an example material with $\omega_0 = 2\pi 0.5\,\text{THz}$, $\omega_p = 2\pi 0.36\,\text{THz}$ and $\gamma = 2\pi 0.01\,\text{THz}$

Before the onset of the resonance, the material behaves as a positive refractive index transmissive material. Then, for roughly the band around resonance ($\omega_0 \pm \gamma/2$), the material behaves as an absorber, reflective after that and for frequencies much higher than the plasma frequency, its transmissive again.

These plots give an insight on the considerations for building a metamaterial based modulator. By dynamically controlling the absorption peak, one can modulate an EM wave passing through the metamaterial around the resonance frequency.

2.3 Metamaterial as a Modulator

As explained in Sect. 1.2.2.2, the electrically coupled LC resonator (ELC) based metamaterial is suitable for planar design since the incident field can be incident to the normal of the device plane. For the ELC resonator shown in Fig. 2.3a, the average permittivity, ignoring the spatial dispersion, is of the Lorentz-like form [17–19]

$$\epsilon_{ELC} = \epsilon_a \left[1 - \frac{Ff^2}{f^2 - f_0^2 + i\gamma f} \right] \tag{2.43}$$

where ϵ_a is the permittivity of the background material, e.g. FR4, GaAs substrate, etc., $f_0 = 1/\sqrt{LC}$ is the resonant frequency in terms of its equivalent circuit parameters (Fig. 2.3b), γ is associated with the loss (R_{loss} in Fig. 2.3b), and F is associated with filing factor of the geometry of the unit cell. The real and imaginary part of the permittivity from Eq. (2.43) is plotted in Fig. 2.3c for an example design with $f_0 = 0.5\,\text{THz}$, $\gamma = 0.01\,\text{THz}$, and $F = 0.5$. The response is similar to the Lorentz oscillator model of non-conductors derived in Eq. (2.32). As observed in Fig. 2.2, the absorption of non-conducting materials is maximum in the vicinity

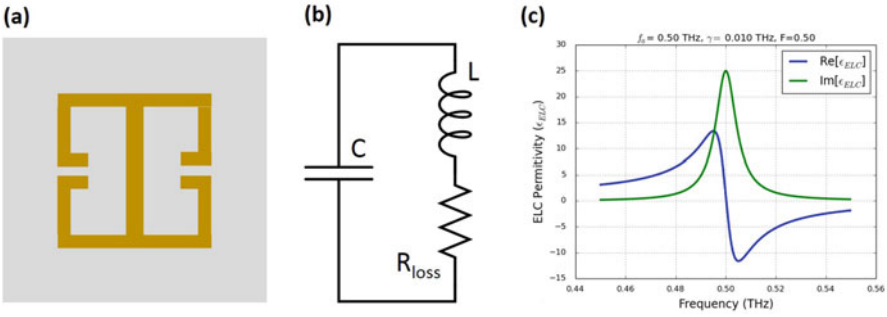

Fig. 2.3 (**a**) An ELC element used in most electric metamaterial design. (**b**) An equivalent circuit of the MM unit cell (**c**) Average permittivity (real and imaginary) of the MM [Eq. (2.43)] for an example design with $f_0 = 0.5\,\text{THz}$, $\gamma = 0.01\,\text{THz}$, and $F = 0.5$

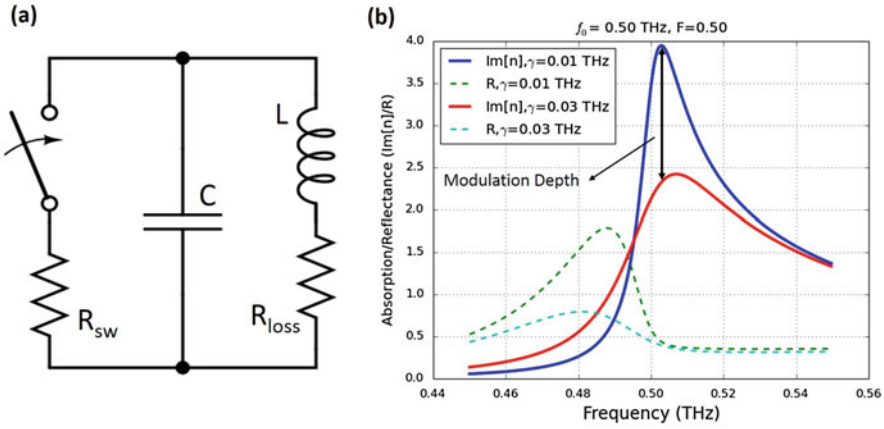

Fig. 2.4 (**a**) A conceptual circuit equivalent of a metamaterial based modulator (**b**) Absorption and reflectance plot of an ELC based metamaterial with and without the modulation resistance (R_{sw})

of molecular resonance frequency. It follows from that observation that, in order to design a metamaterial based modulator for a desired frequency, the resonance frequency of the metamaterial should be designed for that desired frequency and a dynamic method should be devised to either shift the resonance frequency or weaken the resonance by adding loss to the resonator.

One such method is shown conceptually in Fig. 2.4a where a resistive element is used to shunt the MM capacitance of the split gap to weaken the resonance. Assuming the shunt resistor changes the dissipation factor γ from 0.01 to 0.05 THz, the imaginary part of the complex refractive index [n in Eq. (2.39)], which corresponds to the absorption coefficient, is plotted in Fig. 2.4b. It can be seen from the plot that the absorption around the resonance frequency ($f_0 = 0.5$ THz) drops by approximately 40%. The reflectance plot shows little change around the modulation frequency. Terahertz modulators have been demonstrated based on this principle of shunting the split gap capacitance by optically pumping the substrate [20, 21] or electrically injecting carriers [22], a schematic of the basic structure shown in Fig. 1.10. This is the fundamental principle behind the metamaterial based terahertz modulator design in this work that is covered in depth in Chap. 4.

Metamaterial based terahertz modulators have also been demonstrated by dynamically controlling the capacitance or the inductance of the split gap capacitance. A dynamic terahertz metamaterial was realized by dynamically controlling the capacitance of the split gap by optically pumping the substrate and experimentally demonstrated by Chen et al. [23], a schematic of the structure shown in Fig. 1.9. The same work [23] also computationally demonstrated a dynamic terahertz metamaterial by controlling the inductance of the metamaterial unit cell as shown in Fig. 2.5.

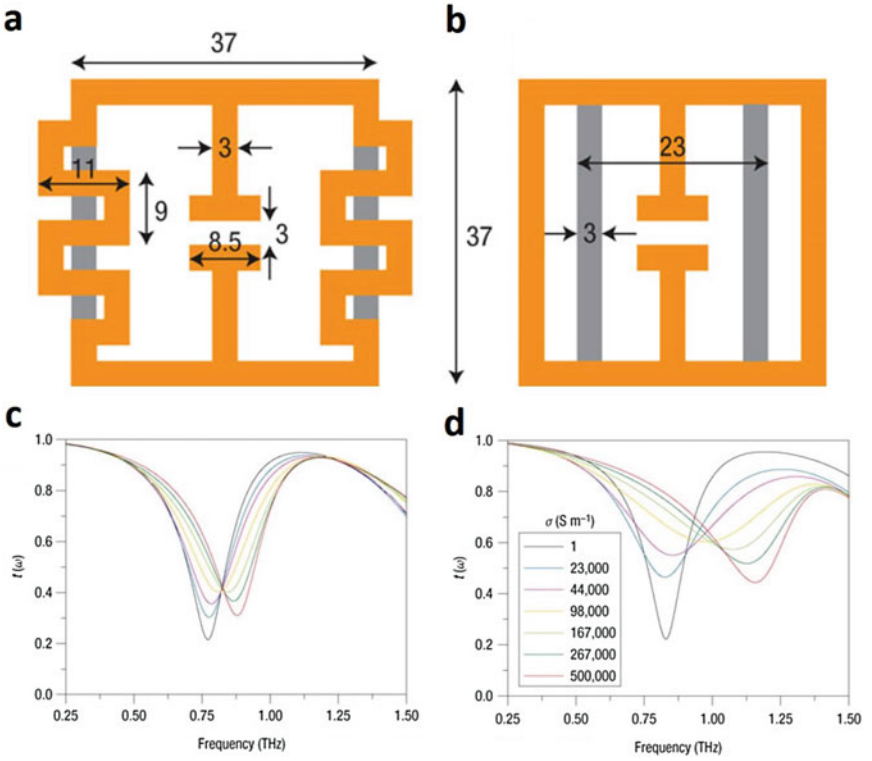

Fig. 2.5 An inductance tune dynamic terahertz metamaterial [23]. (**a**), (**b**) The photoexcited silicon regions form parallel current paths through the meandering loop sections (**a**) and across the regular loop sections (**b**) to effectively modify the inductance of the SRRs. The metal and silicon regions are displayed in *orange* and *grey*, respectively. The dimensions are shown in micrometers. (**c**), (**d**) Simulations of the structure of (**a**) and the structure of (**b**), both using the silicon conductivity values shown in the key

References

1. L.D. Landau, J.S. Bell, M.J. Kearsley, L.P. Pitaevskii, E.M. Lifshitz, J.B. Sykes, *Electrodynamics of Continuous Media* (Elsevier, Amsterdam, 1984)
2. J.D. Jackson, *Classical Electrodynamics*, 3rd edn. (Wiley, New York, 1998)
3. J.A. Kong, *Electromagnetic Wave Theory* (Wiley, New York, 1990)
4. F. Wooten, *Optical Properties of Solids* (Academic, New York, 2013)
5. S.A. Ramakrishna, T.M. Grzegorczyk, *Physics and Applications of Negative Refractive Index Materials* (CRC Press, Boca Raton, 2008)
6. S. Tretyakov, *Analytical Modeling in Applied Electromagnetics* (Artech House, Norwood, 2003)
7. G.V. Eleftheriades, K.G. Balmain, *Negative-Refraction Metamaterials: Fundamental Principles and Applications* (Wiley, New York, 2005)
8. C. Caloz, T. Itoh, *Electromagnetic Metamaterials: Transmission Line Theory and Microwave Applications: The Engineering Approach* (Wiley, New York, 2006)

9. N. Engheta, R.W. Ziolkowski, *Metamaterials: Physics and Engineering Explorations* (Wiley, New York, 2006)
10. J. Pendry, *Fundamentals and Applications of Negative Refraction in Metama* (Princeton University Press, Princeton, 2008)
11. R.W. Ziolkowski, E. Heyman, Phys. Rev. E **64**(5), 056625 (2001)
12. M.W. McCall, A. Lakhtakia, W.S. Weiglhofer, Eur. J. Phys. **23**(3), 353 (2002)
13. V. Veselago, Soviet Phys. Uspekh **10**(4), 509 (1968)
14. I.V. Lindell, S.A. Tretyakov, K.I. Nikoskinen, S. Ilvonen, Microwave Opt. Tech. Lett. **31**(2), 129 (2001)
15. W.J. Padilla, D.N. Basov, D.R. Smith, Mat. Today **9**(7–8), 28 (2006)
16. D.J. Griffiths, *Introduction to Electrodynamics* (Pearson, Boston, 2013)
17. R. Liu, T.J. Cui, D. Huang, B. Zhao, D.R. Smith, Phys. Rev. E **76**(2), 026606 (2007)
18. D.R. Smith, Phys. Rev. E **81**(3), 036605 (2010)
19. B.J. Arritt, D.R. Smith, T. Khraishi, J. Appl. Phys. **109**(7), 073512 (2011)
20. W.J. Padilla, A.J. Taylor, C. Highstrete, M. Lee, R.D. Averitt, Phys. Rev. Lett. **96**(10), 107401 (2006)
21. H.T. Chen, W.J. Padilla, J.M.O. Zide, S.R. Bank, A.C. Gossard, A.J. Taylor, R.D. Averitt, Optics Lett. **32**(12), 1620 (2007)
22. H.T. Chen, W.J. Padilla, J.M.O. Zide, A.C. Gossard, A.J. Taylor, R.D. Averitt, Nature **444**(7119), 597 (2006)
23. H.T. Chen, J.F. O'Hara, A.K. Azad, A.J. Taylor, R.D. Averitt, D.B. Shrekenhamer, W.J. Padilla, Nat. Photon **2**(5), 295 (2008)

http://www.springer.com/978-3-319-52218-0

Active Metamaterials
Terahertz Modulators and Detectors
Rout, S.; Sonkusale, S.
2017, XIII, 118 p. 67 illus., 59 illus. in color., Hardcover
ISBN: 978-3-319-52218-0